# ADVANCED MEASUREMENTS AT THE SPARC PHOTOINJECTOR*

A.Cianchi[a†], D.Alesini[b],A.Bacci[c], M.Bellaveglia[b],R. Boni[b], M.Boscolo[b], M.Castellano[b], L.Catani[a], E.Chiadroni[b], S.Cialdi[c], A.Clozza[b], A. Cook[f],L. Cultrera[b], G.Di Pirro[b], A.Drago[b], M. Dunning[f],A.Esposito[b], D.Filippetto[b], M. Ferrario[b], P. Frigola[f], V.Fusco[b], A.Gallo[b], G.Gatti[b], A.Ghigo[b], L.Giannessi[d],M.Incurvati[b],C.Ligi[b], M.Migliorati[e], A.Mostacci[e], P.Musumeci[f], E.Pace[b],L.Palumbo[e],L.Pellegrino[b], M.Petrarca[g], M.Quattromini[d], R.Ricci[b], C.Ronsivalle[d], J.Rosenzweig[f],A.R.Rossi[c], C.Sanelli[b], L.Serafini[c], M.Serio[b], F.Sgamma[b], B.Spataro[b], F.Tazzioli[b], S.Tomassini[b],C.Vaccarezza[b],M.Vescovi[b],C.Vicario[b]

[a]INFN-Roma "Tor Vergata", via della Ricerca Scientifica, 1 - 00133 Rome, Italy

[b]INFN-LNF, via E. Fermi, 40 - 00044 Frascati, Rome, Italy

[c]INFN-Milano, Via Celoria 16, 20133 Milan, Italy, [d]ENEA, via E. Fermi, 00044 Frascati, Rome, Italy

[e]Università di Roma "La Sapienza", Dip. Energetica, via A. Scarpa, 14 - 00161, Rome, Italy

[f]UCLA - Dept. of Physics and Astronomy, 405 Hilgard Avenue, Los Angeles, California 90095, USA

[g]INFN-Roma I, p.le A. Moro 5, 00185 Roma, Italy

*Abstract*

The goal of the first stage of the SPARC commissioning was the optimization of the RF-gun settings that best match the design working point. This entailed detailed study of the emittance compensation process providing the optimal value of emittance at the end of the linac. For this purpose an innovative beam diagnostic, the emittance-meter [1], consisting of a movable emittance measurement system, was conceived and built. More than a simple improvement over conventional, though non-trivial, beam diagnostic tools this device defines a new strategy for the characterization of new high performance photo-injectors. The emittance meter allows measurements at different locations along the beamline of the evolution of important beam parameters both in longitudinal and in the transverse phase spaces. These parameters, which include such as beam sizes, energy spread and rms transverse emittances, are measured in a region where the space-charge effects dominate the electron dynamics. The quality and the quantity of the data allowed a clear reconstruction of the phase space evolution. We report also the first experimental observation of the double emittance minima effect up on which the optimized matching with the SPARC linac is based.

## INTRODUCTION

The SPARC [2] project is an R&D photo-injector directed towards production of high brightness electron beam that is able to drive a SASE-FEL experiment. The 150 MeV SPARC photo-injector consists of a 1.6 cell RF gun operated at S-band (2.856 GHz, of the BNL/UCLA/SLAC type) and high-peak field on the cathode incorporated metallic photo-cathode of 120 MV/m [3], generating a 5.6 MeV, 100A (1 nC, 10 ps) beam.

The beam is then focused and matched into 2 SLAC-type accelerating sections, which boost its energy to 150-200 MeV. SPARC is also the prototype of the recently approved SPARX project that foresees the construction of a new high brightness electron linac for producing SASE-FEL radiation with wavelengths in the range of 10-1.5 nm.

The first phase of the SPARC Project has been dedicated to the complete characterization of the beam parameters, at different distances from the photocathode, to find the injector settings optimizing emittance compensation and to make code validation.

The possibility of measure beam parameters at different *z* position (being *z* the longitudinal distance from the cathode) was considered fundamental to allow a complete reconstruction of the evolution of these parameters and to make extensive studies on the beam dynamics.

## EMITTANCE-METER

To make measurement in different z positions, a dedicated movable emittance measurement device (emittance-meter) was used. This device allowed measurement of beam parameters in the range from about *z*=1000 mm to *z*=2100 mm.

The technique of measuring the beam emittance and the phase space, in both the horizontal and vertical planes, makes use of a double system of horizontal and vertical slit masks [4].

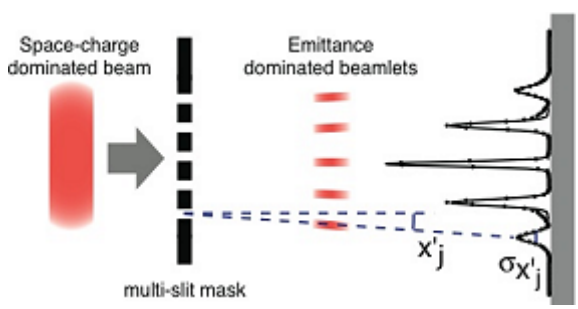


Figure 1: technique

* partially supported by the EU Commission in the FP6 program, Contract No. 011935 EUROFEL-DS1

† cianchi@roma2.infn.it

Selecting an array of beamlets by means of an intercepting multi-slit mask, alternatively creating one beamlet using a single slit moving transverse over the beam spot, reduces the space charge dominated incoming beam into emittance-dominated beamlets that drift up to an intercepting screen(see Fig. 1). If the screen response is linear, the intensity of beamlets spots on the screen are directly proportional to the number of particles in the beamlets which hit the screen. The emittance can be retrieved calculating the second momentum of the beam as reported in [5]. The slits mask must stop, or largely degrade, the intercepted components of the beam , while avoiding excessive slit-scattering effects. A 2 mm thick tungsten is used for the mask.

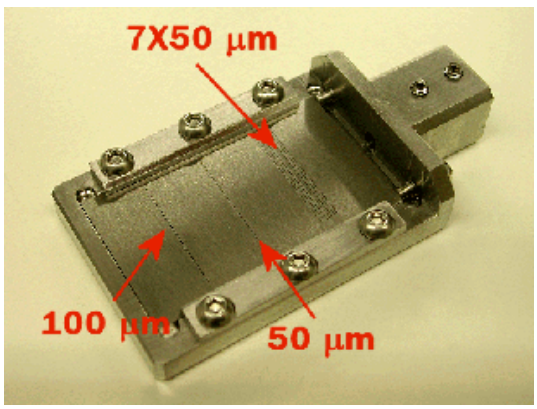


Figure 2: Mask layout

Along the beam trajectory spanned by the emittance meter the beam changes from converging to diverging as it undergoes a space-charge dominated waist. For this reason some flexibility was built into the diagnostic, by using different inter-slit spacing for different conditions.

To this end each mask consists of a slit array(7 slits, 50 $\mu$m width spaced of 500 $\mu$m, 2 mm thick) and two single slits, 50 and 100 $\mu$m width(see Fig. 2). The slits are fabricated by electro-chemical etching, which provides, in comparison to mechanical machining, higher precision and improved smoothness of the slit edges. Each individual slit was machined as a component of 0.5 mm height and later assembled into the frame. This configuration allows the geometry of the slit mask to be changed by simply reorganizing the component pieces.

The multi-slit mask was used for single shot measurements, when the beam size was large enough for an adequate beam sampling by the slit array. Alternatively, a single slit was moved across the beam spot in a multi-shot measurement. In this case the accuracy of transverse sampling can be freely chosen adjusting the step between the different positions of the slit. Typical values of the sampling distance between the slit positions ranges from 110 $\mu$m to 380 $\mu$m Between nine and thirteen beamlets are collected in the single slit scans. No relevant differences were found between results obtained using single or multislits techniques in cases where comparison was possible. Because the accuracy of the phase space reconstruction is much better with single slit and it further gives also the flexibility of changing the relative distance between the beamlets, it was usually employed.

Linear actuators with stepper motors were used to move the slits masks into the beamline. A differential encoder and a reference end switch guarantees reproducibility and accuracy of the movement to better than 2 $\mu$m, as required for single-slit multi-shots measurements.

The beamlets emerging from the slit-mask are measured by means of a downstream Ce:YAG radiator. Because beam size and divergence depend on the device's longitudinal position, the slit to screen distance must be properly adjusted in order to optimize the accuracy of the beamlet profiles measurement. A bellow is therefore placed (see Fig. 3) in between the slit mask and the screen, allowing their relative distance to be changed from 22 to 42 cm, to optimize the drift in order to accomodate several scenarios (converging beam, diverging beam, single or multi-slits).

Radiation emitted in the forward direction from the Ce:YAG crystal is collected by a 45 degrees mirror just downstream of the radiator, and attached to the same screen holder. The back face of the transparent crystal radiator is observed, thus minimizing degradation of the spatial resolution due to the depth of field of the optics. The small thickness of the crystal (100 $\mu$m) prevents appreciable blurring effect, due to bulk emission, as well as significant multiple scattering. A calibration grid, with 2 mm wire spacing, is also machined to the same frame holder of the YAG crystal, allowing in situ calibration.

Images are acquired using digital CCD cameras (Basler 311f) equipped with simple 105mm "macro" type objectives from SIGMA. The magnification used of about 0.66 gives a calibration near to 15 $\mu$m per pixel and a field of view of the screen around 9.6 X 7.2 mm.

Such cameras offer the advantage that the signal is digitalized directly by on-board electronics so that there is no need for a frame grabber and the output signal, being digital, is less sensitive to environmental noise. The IEEE1394 (Firewire) link allows simpler cabling topology because it carries both pixel readouts and commands to the camera. The Firewire cable from every CCD is connected to a front end industrial PC inside the accelerator tunnel running windows XP.

LabVIEW$^{TM}$ software was used for DAQ and control because of its simplicity in accomodating hardware connections, data acquisition and manipulation. There are drivers available for Firewire interface using LabVIEW$^{TM}$ only under Windows XP. The data are collected by the industrial PC and sent to a central server that is the basis of the SPARC control system [6].

The overall system is similar to the optical diagnostic system that we've realized at FLASH [7], with the extension of the connection topology to all devices in the tunnel hall. The camera system applications software and the configuration files are made available to the camera controllers from a shared network disk hosted by the central server.

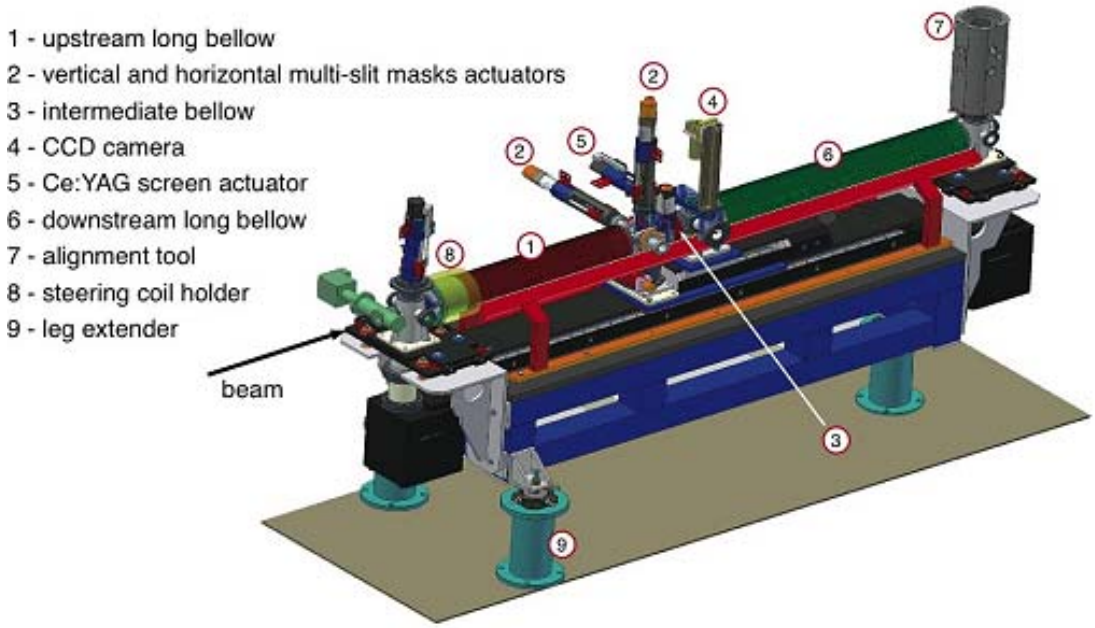


Figure 3: 3D drawings of the emittance meter

This simplifies greatly the installation and maintenance of all hardware devices.

The emittance-meter is followed by a magnetic spectrometer which measures the beam energy and energy spread. The charge is measured by means of ICT placed in the spectrometer area.

The influence on the beam quality of the 1.5 m long bellow has been investigated [8]. Wake field perturbations due to the corrugated structure, especially when beam is not well-aligned on-axis, were studied using HOMDYN code and the wake fields were computed with the diffractive model of Bane and Sands [9]. In the worst case of 1 mm misalignment the contribution of the wakes to the emittance degradation is practically negligible.

## RESULTS

In the early runs of SPARC the laser illuminated the photocathode through the 72 degrees view port built in the gun. The results of this run has been already reported in [10] and will not be discussed here. To decrease the laser energy lost in the light transport, and to improve the laser spot transverse uniformity, a simpler scheme using quasi-normal incidence on the photocathode has been adopted.

### *Beam envelope*

The measure of the beam envelope is central finding the position of the beam waist, comparing it to the expected position, and benchmarking the field strength of the solenoid.

The emittance meter allows meaurements of the beam envelope at different $z$ positions by simply moving from one position to other, collecting images and averaging over several shots.

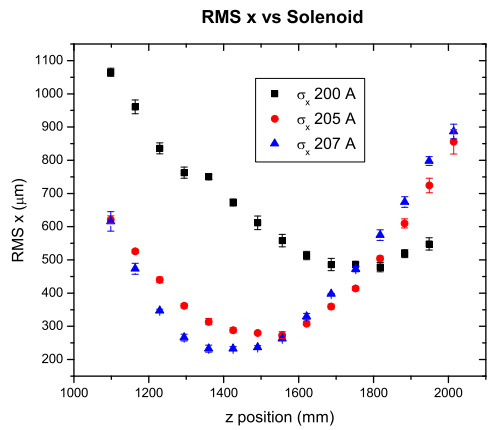


Figure 4: Several rms beam size measurements with different solenoid field

The envelope measurement is a critical input for benchmarking simulations because it provides additional information on the beam dynamics that aid in the reconstruction of the beam evolution.

### *Emittance*

The measurement of the emittance evolution along the photoinjector was the main goal of the diagnostic. Several runs were dedicated to comparison of the dynamics of the beam under different conditions: moving the injection phase, changing the solenoid strength, and varying the longitudinal profile of the laser. Fig. 5 shows a measurement with a flat top longitudinal beam profile, 9 ps FWHM,

with rise time of about 2.5 ps and nominal current of 92A. The solid line is the result of a PARMELA [11] simulation using actual beam parameters, such as laser pulse length, beam size, launch phase and so on.

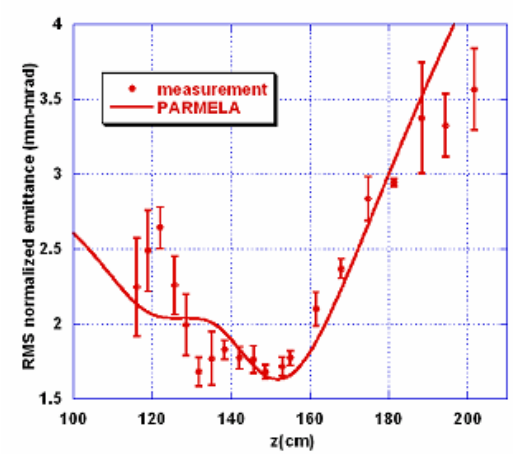


Figure 5: Emittance evolution of high brightness beam. The solid line is a PARMELA simulation

The agreement between the measurements and the simulation is very good. It must be stressed that these are the first experiments ever performed in which the beam emittance evolution in $z$ was measured. Until now, the only possibility was to measure the emittance and the beam size at a fixed position in $z$. By variation of the beam parameters it was possible to move the solid line in Fig. 5 over the position where the measurements were done. Unfortunately this approach has the disadvantage that the curve doesn't move rigidly, so a certain number of assumption must be made in order to interpret the data and benchmark the experiment with the simulation. With the emittance meter there is a direct measurement of the emittance evolution, and no assumptions are required. Fig. 6 shows the comparison between a flat top longitudinal pulse with 85A current 8.5 ps length, 2.5 ps rise time, and a gaussian beam with the same FWHM length.

The emittance oscillation observed in simulation of the photoinjector is a notable feature of the Ferrario working point [12], the most common emittance compensation design now employed in photoinjectors worldwide. This effect is quite small and is enhanced both by fast laser rise time and high energy spread. We have obtained a direct evidence of this type of double minimum oscillation working with very small laser rise time ($\cong$ 1.5 ps) and moving the phase toward the crest of the RF, even if the minimum achievable value of the emittance is larger in this case.

### *Phase space*

The technique used to measure the emittance allows the phase space sampling. Using a large number of samples (13 moving the single slit over the beam) it's possible to reconstruct the beam transverse phase space and follow its evolution, as shown in Fig. 8.

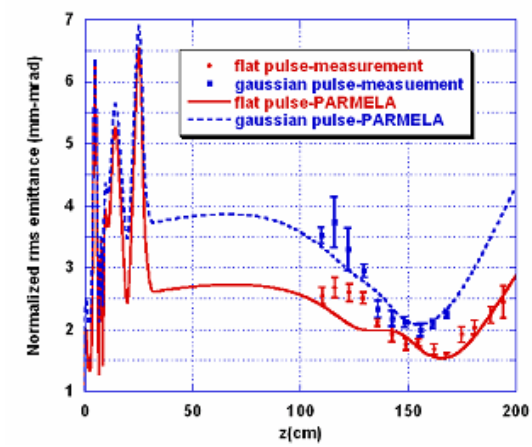


Figure 6: Comparison between the emittance vs z of two different beams: longitudinal flat top with rise time of 2 ps and gaussian profile with the same FWHM of 8.5 ps.

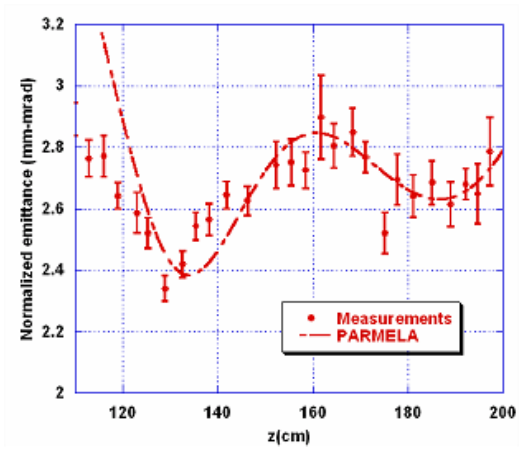


Figure 7: The first direct evidence of a double minimum oscillation of the emittance in a photoinjector

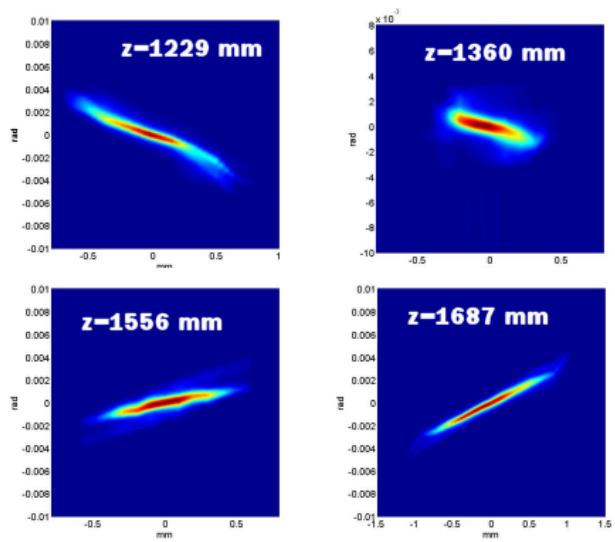


Figure 8: Reconstructed phase space for different z position

In addition to being a visual aid in understanding the beam dynamics, the phase space contains valuable information. A new algorithm has been developed to calculate the value of the emittance using the phase space data. The agreement with a traditional algorithm starting from the beamlets images [13] is excellent [14].

### *Energy spread*

After the tungsten mask the emerging beamlets are not longer space charge dominated. The contribution of the space charge to the energy spread is also frozen.

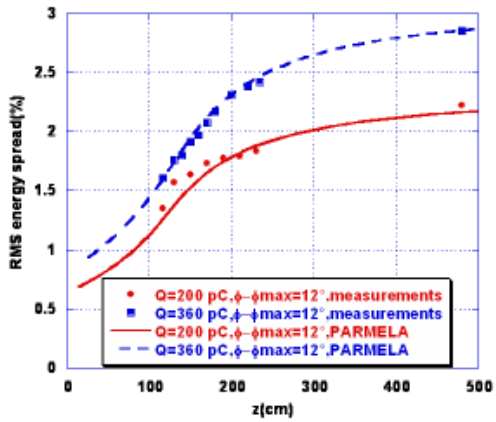


Figure 9: Energy spread vs z for two different bunch current

In Fig. 9 a measure of the energy spread obtained by collimating the beam with one slit at different $z$ positions for two different current, along with the preditions of PARMELA simulations. Because in the fit model there is no contribution from the long emittance meter bellows, it was possible to confirm that the effect of the bellows is negligible. Also this gives information on the longitudinal phase space of the beam.

## CONCLUSIONS

The SPARC emittance meter gives the possibility of measuring the beam parameters at different distances from the cathode, giving information on the transverse and longitudinal phase spaces. Improvement in the laser parameters, changes in the solenoids field, and modifications in the solenoid alignment can be easily and quickly checked. Also the possibility of having several measurements along the beam line gives a better understanding of the dynamics and a more direct comparison with the simulations. The agreement between the measurement and the simulations is excellent, due to the large number of the samples taken, as well as to the cross check provided by the envelope measurement. The high sampling rate of the phase space also allows running tools directly on it to evaluate the value of the emittance.

Finally, we note that the measurement of the double minimum in the emittance oscillation provides a direct validation of the theory behind the choice of the Ferrario's working point.

### *Acknowledgment*

The authors wish to thank all SPARC collaboration scientists and engineers who contributed to the design and commissioning of the emittance meter. Special thanks to V. Lollo for his contribution to the system mechanical design, engineering, and bench testing, F. Anelli and S. Fioravanti for their work on motor controllers. Also thanks to A. Battisti, L. Antonio and S. Stabioli

This work has been partially supported by the EU Commission in the sixth framework program, Contract No. 011935 EUROFEL-DS1.

## REFERENCES

[1] L. Catani et al."'Design and characterization of a movable emittance meter for low-energy electron beams"',Review of Scientific Instruments 77, 093301 2006

[2] D. Alesini et al., Nucl. Instr. & Meth. In Phys. Res. A 507 (2003) 345-349C

[3] J.B. Rosenzweig, A.M. Cook, M.P. Dunning, P. Frigola, G. Travish, C. Sanelli, F. Tazzioli, D.T. Palmer,'RF and magnetic measurements on the SPARC photoinjector and solenoid at UCLA', Proceedings of the PAC 2005,Knoxville (USA), pag 2624 - 2626

[4] S.G. Anderson, J.B. Rosenzweig, G. P. Le Sage, J.K. Crane, Space-charge effects in high brightness electron beam emittance measurements, Phys. Rev. ST Accel Beams 5, 014201 (2001)

[5] Claude Lejeune and Jean Aubert, Adv. Electron. Electron Phys., Suppl. 13A, 159 (1980).

[6] M. Bellaveglia et. al "'SPARC control system"' Proceedings of PCAPAC2005, Hayama,Japan

[7] L. Catani, A. Cianchi, G. Di Pirro,K. Honkavaara "A large distributed digital camera system for accelerator beam diagnostics",Review of Scientific Instruments 76, 073303 (2005)

[8] V. Fusco et al., "Wake Fields Effects in the Photoinjector of the SPARC Project", Proceedings of EPAC2004, Lucerne, Switzerland pag.405

[9] K. Bane, M. Sands, SLAC-Pub-4441

[10] A. Cianchi et al.,"Characteriztion of the SPARC Photo-injector movable emittance meter",Procceding of EPAC2006,Edinburgh, Scotland (2006), pag 3523

[11] L. M. Young, PARMELA, Los Alamos National Laboratory report LA-UR-96-1835

[12] M. Ferrario, J. E. Clendenin, D. T. Palmer, J. B. Rosenzweig, L. Serafini,"Homdyn study for the LCLS RF photoinjector",SLAC-PUB 8400

[13] D. Filippeto et al "Robust alghoritm for slit emittance measurement", SPARC-note to pe published

[14] A.Cianchi et al. "Accurate emittance calculation from phase space analysis", SPARC-note to be published